INFLUENCE OF PHYSICO-CHEMICAL MATERIAL CHARACTERISTICS ON STAPHYLOCOCCAL BIOFILM FORMATION – A QUALITATIVE AND QUANTITATIVE *IN VITRO* ANALYSIS OF FIVE DIFFERENT CALCIUM PHOSPHATE BONE GRAFTS

M. Clauss[1,2,3,*], U. Furustrand Tafin[4], B. Betrisey[3], N. van Garderen[2], A. Trampuz[3,5], T. Ilchmann[1] and M. Bohner[2]

[1]Clinic for Orthopaedics and Trauma Surgery, Kantonsspital Baselland, Liestal, Switzerland
[2]RMS Foundation, Bettlach, Switzerland
[3]Infectious Diseases Service, Department of Internal Medicine, University Hospital Lausanne (CHUV), Lausanne, Switzerland
[4]Septic Surgical Unit, University Hospital Lausanne (CHUV), Lausanne Switzerland
[5]Department for Traumatology and Reconstructive Surgery, Charité, Berlin, Germany

Abstract

Various compositions of synthetic calcium phosphates (CaP) have been proposed and their use has considerably increased over the past decades. Besides differences in physico-chemical properties, resorption and osseointegration, artificial CaP bone graft might differ in their resistance against biofilm formation. We investigated standardised cylinders of 5 different CaP bone grafts (cyclOS, chronOS (both *β-TCP* (tricalcium phosphate)), dicalcium phosphate (DCP), calcium-deficient hydroxyapatite (CDHA) and α-TCP). Various physico-chemical characterisations *e.g.*, geometrical density, porosity, and specific surface area were investigated. Biofilm formation was carried out in tryptic soy broth (TSB) and human serum (SE) using *Staphylococcus aureus* (ATCC 29213) and *S. epidermidis* RP62A (ATCC 35984). The amount of biofilm was analysed by an established protocol using sonication and microcalorimetry. Physico-chemical characterisation showed marked differences concerning macro- and micropore size, specific surface area and porosity accessible to bacteria between the 5 scaffolds. Biofilm formation was found on all scaffolds and was comparable for α-TCP, chronOS, CDHA and DCP at corresponding time points when the scaffolds were incubated with the same germ and/or growth media, but much lower for cyclOS. This is peculiar because cyclOS had an intermediate porosity, mean pore size, specific surface area, and porosity accessible to bacteria. Our results suggest that biofilm formation is not influenced by a single physico-chemical parameter alone but is a multi-step process influenced by several factors in parallel. Transfer from *in vitro* data to clinical situations is difficult; thus, advocating the use of cyclOS scaffolds over the four other CaP bone grafts in clinical situations with a high risk of infection cannot be clearly supported based on our data.

Keywords: Biofilm; calcium phosphate; β-TCP; *S. aureus* ATCC 29213; *S. epidermidis* RP62A ATCC 35984; microcalorimetry; sonication; bone graft.

*Address for correspondence:
Martin Clauss
Kantonsspital Baselland Liestal,
Clinic for Orthopaedics and Trauma Surgery
Rheinstrasse 26
CH-4410 Liestal, Switzerland
Telephone Number: +41 61 925 3722
FAX Number: +41 61 925 2808
Email: martin.clauss@ksbl.ch

Introduction

More than one million patients per year need a bone grafting procedure to repair a bone defect resulting from a trauma or a bone disease. The use of autologous cancellous bone grafts transplanted as fresh bone grafts is regarded as the gold standard (Delloye *et al.*, 2007; Ketonis *et al.*, 2010). However, several bone graft substitutes have been proposed, such as fresh-frozen allogeneic cancellous bone grafts (Van de Pol *et al.*, 2007; Kappe *et al.*, 2010) and processed human or bovine cancellous bone grafts (Tadic and Epple, 2004). All these genuine bone grafts have a comparable calcium phosphate (CaP) architecture (Clauss *et al.*, 2013). In the 1970s, various compositions of synthetic CaP, such as β-tricalcium phosphate (β-TCP) or hydroxyapatite (HA), were proposed. Their importance and use have considerably increased over the past decades (Bohner, 2000). Their subtle differences in composition and structure may have a profound effect on their *in vivo* behaviour (Bohner, 2000). Besides differences in chemical properties, resorption and osseointegration, artificial bone graft might differ in case of bacterial colonisation and biofilm formation.

Surgical site infection is a recognised and often devastating complication in orthopaedic surgery ranging from 0.7-4.2 % in elective orthopaedic surgery (Crockarell *et al.*, 1998) to 30 % following third degree open fractures (Ostermann *et al.*, 1994). *S. aureus* and *S. epidermidis* are the main microorganisms responsible for 60-80 % of these infections (Gristina, 1987; Trampuz and Zimmerli, 2006b). Despite antimicrobial prophylaxis in modern operating rooms, surgical site infections cannot be completely prevented (Trampuz and Zimmerli, 2006a), especially in the vicinity of a foreign body (Busscher *et al.*, 2012). Bacteria are growing attached to the surface as biofilm (Costerton *et al.*, 2005; Trampuz and Zimmerli, 2006b). The treatment and eradication of infections caused by biofilms is more difficult than of bacteria growing in free-living (planktonic) form (Busscher *et al.*, 2012). The eradication of infection is often only possible by removal of the foreign body and long-term antimicrobial treatment (Ehrlich *et al.*, 2005).

The "race to the surface" (Gristina, 1987) as a multistep process of initial bacterial adhesion and later biofilm formation is well established for metal implants (Gristina, 1987; Oga *et al.*, 1988; Cordero *et al.*, 1994; Vogely *et al.*, 2000; Harris and Richards, 2006; Schlegel and Perren, 2006; Harris *et al.*, 2007). In contrast, there

are only limited data on biofilm formation on the surface of different CaP bone graft substitutes, mainly HA and tricalcium phosphate (Van Blitterswijk *et al.*, 1986a; Van Blitterswijk *et al.*, 1986b; Van Blitterswijk *et al.*, 1986c; Jakubowski *et al.*, 2008; Westas *et al.*, 2014). Considering their increasing use in orthopaedic surgery, there might be more infected bone grafts in the future and differences in initial adhesion and biofilm formation might have a direct impact on clinical infection rates. Therefore, the aim of this study was to analyse the influence of material properties of 5 different synthetic CaP bone grafts on the initial adhesion and biofilm formation in an established *in vitro* setting (Clauss *et al.*, 2010) using standard laboratory strains of *S. aureus* and *S. epidermidis* which are commonly causing surgical site bone infection.

Material and Methods

Four out of 5 examined CaP scaffolds used in the present study were produced using the so-called calcium phosphate emulsion method (Bohner, 2001; Kasten *et al.*, 2003; Bohner *et al.*, 2005). In brief, a powder mixture consisting of 80 g of α-tricalcium phosphate (α-TCP; α-$Ca_3(PO_4)_2$; produced in-house) and 20 g of tricalcium phosphate (Merck, Dietikon, Switzerland) was mixed with 100 g viscous paraffin oil (Merck) and 60 mL of 0.2 M Na_2HPO_4 aqueous solution containing 0.57 g/L of polyethoxylated castor oil (Cremophor EL, BASF, Wädenswil, Switzerland), and 1 % of 5.1 kDa poly(acrylic acid) (Fluka, Buchs, Switzerland). After 2 min of mixing at 2000 rpm, the paste was poured into standing 30 mL syringes the tip of which had been pre-cut. Fourty-five minutes later, the samples were covered with 10 mL phosphate buffer (phosphate-buffered saline, PBS) (4.5 g/L NaCl, 1.79 g/L KH_2PO_4, 9.0 g/L $Na_2HPO_4 \cdot 2H_2O$), and incubated for one day at 60 ºC. Then the samples were incubated in petroleum ether, dried and sintered at 1250 ºC. After drying, the samples were lathed to obtain the desired block dimensions. The last processing steps included a cleaning stage in ethanol and final calcination at 900 ºC for 1 h.

The samples obtained according to this procedure consisted of pure β-tricalcium phosphate (β-TCP; β-$Ca_3(PO_4)_2$, named here "chronOS" due to their similarity to the product sold by DePuy Synthes (West Chester, PA, USA). To obtain α-TCP scaffolds, the β-TCP scaffolds (chronOS) were calcined at 1500 ºC for 12 h and rapidly cooled down to room temperature. The conversion of α-TCP scaffolds into dicalcium phosphate scaffolds (DCP; $CaHPO_4$) occurred *via* a chemical reaction between α-TCP scaffolds and a phosphoric acid solution (Galea *et al.*, 2008).

For the synthesis of calcium-deficient hydroxyapatite (CDHA; $Ca_9(PO_4)_5(HPO_4)(OH)$), calcium phosphate emulsions were also used (Kasten *et al.*, 2003). Compared to the synthesis of β-TCP scaffolds, polyacrylic acid was replaced by sodium citrate (0.2 M concentration) and the fraction of emulsifier was reduced from 0.57 to 0.40 g/L. The incubation at 60 ºC lasted 72 h instead of 24 h and the samples were cleaned with petroleum ether in a soxhlet device (VELP Scientifica, Usmate, Italy). The samples were not sintered.

The fifth CaP material (named here "cyclOS") was a β-TCP scaffold which was purchased at Mathys Ltd (Bettlach, Switzerland). According to the producer, these materials were obtained by pressing a mixture of tricalcium phosphate powder and polymer beads (125-625 µm), followed by sintering at 1100 ºC.

Physico-chemical characterisation

Various physico-chemical characterisations were performed on all the investigated scaffolds: measurement of their weight, diameter, and height to determine their geometrical density and porosity, X-ray diffraction (XRD) to determine their crystalline composition, Nitrogen adsorption to determine their specific surface area (SSA) using the BET model, mercury porosimetry to determine their microstructure in the range between 7 nm and 100 µm using the Washburn equation, scanning electron microscopy (SEM) and optical microscopy to look at their morphology and estimate the macropore size (pore size > 50-100 µm). More details are provided below.

The geometrical density was determined by dividing the weight by the apparent volume of the scaffolds. For XRD the scaffold was crushed, homogenised and packed in a cavity in an aluminium sample holder. XRD data were collected in reflective geometry on a Panalytical CubiX diffractometer (Panalytical, Eindhoven, The Netherlands) equipped with a graphite monochromator in the secondary beam. CuKα radiation and a step size of 0.02° were used to measure from 4.01 to 59.99° 2θ. Quantitative phase analysis was done by Rietveld refinement with the computer program FullProf.2k (Version 5.00) (Rodriguez-Carvajal, 2001), using a previously determined instrument resolution function. Starting models for the quantified phases were taken from Dickens *et al*. (Dickens *et al.*, 1974) for β-TCP, Mathew *et al*. (Mathew *et al.*, 1977) for α-TCP, Sudarsanan and Young (Sudarsanan and Young, 1969) for hydroxyapatite, Dickens *et al*. (Dickens *et al.*, 1971) for DCP, and Curry and Jones (Curry and Jones, 1971) for dicalcium phosphate dihydrate (DCPD; $CaHPO_4 \cdot 2H_2O$). The SSA was measured by nitrogen adsorption using the BET model (Gemini 2360, Micromeritics, Norcross, GA, USA). Four measurements were made per material. Total porosity and pore size distributions were evaluated with a mercury porosimeter up to 200 MPa (Pascal 140/440, Thermo Fisher, Schwerte, Germany). Surface tension and contact angle of mercury were set to 0.480 N/m and 140°, respectively. Samples were dried overnight at 130 °C in order to drive off any physisorbed water from the sample. Three different samples were measured to determine the standard deviation. For SEM, broken pieces of the scaffolds were placed on a sticky carbon tape, itself sticking on an aluminium sample holder. The particles were then sputtered with C and subsequently with Au to a total thickness of approximately 20 nm. The samples were observed with an EVO MA25 microscope (Zeiss, Oberkochen, Germany). The macropore size of the samples was estimated by optical microscopy using a method previously described (Bohner *et al*., 2001). Briefly, photos of the surface of polished and cleaned scaffolds were taken (Leica (Wetzlar, Germany).

MZ12 microscope, JVC KY-F70 digital camera, Image Access software). The average diameter of fifteen macropores was determined and an average macropore diameter, D_e, was calculated. The final macropore diameter, D, was calculated from D_e using equation (1) (assuming that all the macropores are round and homogeneously distributed):

$$D = \sqrt{\frac{3}{2}} D_e \quad (1)$$

Biofilm formation

Two established biofilm forming staphylococcal strains were used (Clauss *et al.*, 2010): *S. aureus* (ATCC 29213) is a gram-positive, coagulase-positive, methicillin-susceptible, biofilm-forming strain (Ceri *et al.*, 2001). *S. epidermidis* RP62A (ATCC 35984) is a gram-positive, coagulase-negative, biofilm-forming strain (Merritt *et al.*, 1998). The strains were stored at -70 °C by using a cryovial bead preservation system (Microbank, Por. Lab Diagnostics, Richmond Hill, Ontario, Canada). For preparation of the inoculum, a single bead was freshly grown on sheep blood agar overnight. Bacterial inocula were prepared from discrete colonies resuspended in 1 % PBS to a McFarland turbidity of 0.5 representing a bacterial concentration of ~1.0 x 10^8 colony-forming units (cfu)/mL. The stock solution was diluted 1:1.000 for further experiments.

Biofilm formation was performed in (i) tryptic soy broth (TSB, Beton Dickinson AG, Basel Switzerland) and (ii) undiluted pooled human serum (serum, Millipore™ Temecula CA, United States) as recently published (Clauss *et al.*, 2010). In brief, CaP bone grafts were inserted in 50 mL-Falcon tubes pre-filled with 2700 µL of medium. To allow a homogeneous soaking of the porous materials over a 30 min period, samples were placed on top of the liquid surface (Stähli *et al.*, 2010). At the end of the period, samples were completely submerged due to the additional water content in the pores (Clauss *et al.*, 2013). In a final step, 300 µL of diluted bacterial stock solution were added resulting in an initial bacterial concentration of *S. aureus* of ~1.5 x 10^5 cfu/mL, and for *S. epidermidis* ~1.0 x 10^5 cfu/mL. Samples were incubated under static conditions at 37 °C with ambient air for either 3 h, 24 h or 72 h.

Biofilm analysis was adapted from our recently published procedure (Clauss *et al.*, 2010). Three steps were included: (i) washing procedure (all samples) followed by (ii) sonication (half of the samples) and (iii) a final microcalorimetric analysis (all samples).

(i) *Washing procedure*: After incubation, CaP scaffolds were transferred to a new 50 mL-Falcon tube (prefilled with 5 mL 1 % PBS) with a sterile forceps. They were washed 5 times with 5 mL 1 % PBS to remove planktonic bacteria. For washing the PBS was poured in the Falcon tubes by placing a glass pipette on the wall of the Falcon tubes; afterwards the Falcon tubes were shaken cautiously by hand, and in a final step the PBS was sucked-off by placing a Pasteur pipette on top, to one side of the CaP scaffolds, to have a flush through the scaffold. Both the glass pipette and the Pasteur pipette were changed after processing one scaffold, to avoid contamination from one sample to another. Afterwards samples were split in two groups for further analysis: Group A was analysed by microcalorimetry alone and group B by sonication and microcalorimetry.

(ii) *Sonication procedure (only group B)*: After washing, samples were transferred to new 50 mL-Falcon tubes containing 5 mL 1 % PBS, gently shaken for 5 s, sonicated at 40 kHz for 5 min in a bath tub sonicator (BactoSonic, Bandelin, Germany) and shaken again for 5 s. The dislodged biofilm (sonication fluid) was transferred to a 10 mL-Falcon tube and CaP bone grafts were stored for microcalorimetry (see below).

Sonication fluid was serially diluted in Eppendorf tubes and aliquots of 100 µL were plated on sheep blood agar and incubated at 37 °C aerobically for 24 h. Bacterial counts were enumerated and expressed as cfu/sample. Plates were examined for variations in colony morphology (colour, size) and contaminations.

(iii) *Microcalorimetry protocol (group A and B)*: all microcalorimetry tests were performed using a 48-channel batch calorimeter (thermal activity monitor, model 3102 TAM III; TA Instruments, New Castle, DE, USA).

In more detail, biofilm-loaded CaP samples were transferred into sterile 4 mL calorimeter ampoules pre-filled with 1 mL TSB, closed with a rubber cap and sealed by manual crimping. Ampoules were sequentially introduced into the microcalorimeter and remained for 15 min in the thermal equilibration position before they were lowered into the measurement position. Heat flow was measured continuously after the signal stability was achieved throughout an 18 h period and expressed as heat flow over time (in microwatts [µW]). The calorimetric time to detection (TTD) was defined as the time from insertion of the ampoule into the calorimeter until the exponentially rising heat flow signal exceeded 50 µW to distinguish microbial heat production from the thermal background. TTD indirectly quantifies the amount of bacteria with a shorter TTD representing a larger amount of bacteria. Data analysis was accomplished using the manufacturer's software (TAM Assistant; TA Instruments) and Prism 5.0 (GraphPad Software, La Jolla, CA).

Statistical calculations

Physico-chemical characterisation was done with at least three scaffolds of each material. Data are presented as mean and standard deviation (SD).

Biofilm experiments were performed in triplicates. To equalise variances in bacterial counts, data are presented as $\log_{10}$ cfu/sample. For statistical analysis a one-way ANOVA with Bonferroni's multiple comparison test was performed using Prism 5.0 (GraphPad Software, La Jolla, CA). A p-value of < 0.05 was considered to be significant.

Results

Material characteristics

Apart from the DCP samples, all scaffolds had a purity close to 100 % (Table 1). The DCP scaffolds contained about 6 % of remaining or unreacted α-TCP. All samples contained large pores (macropores) with a diameter close

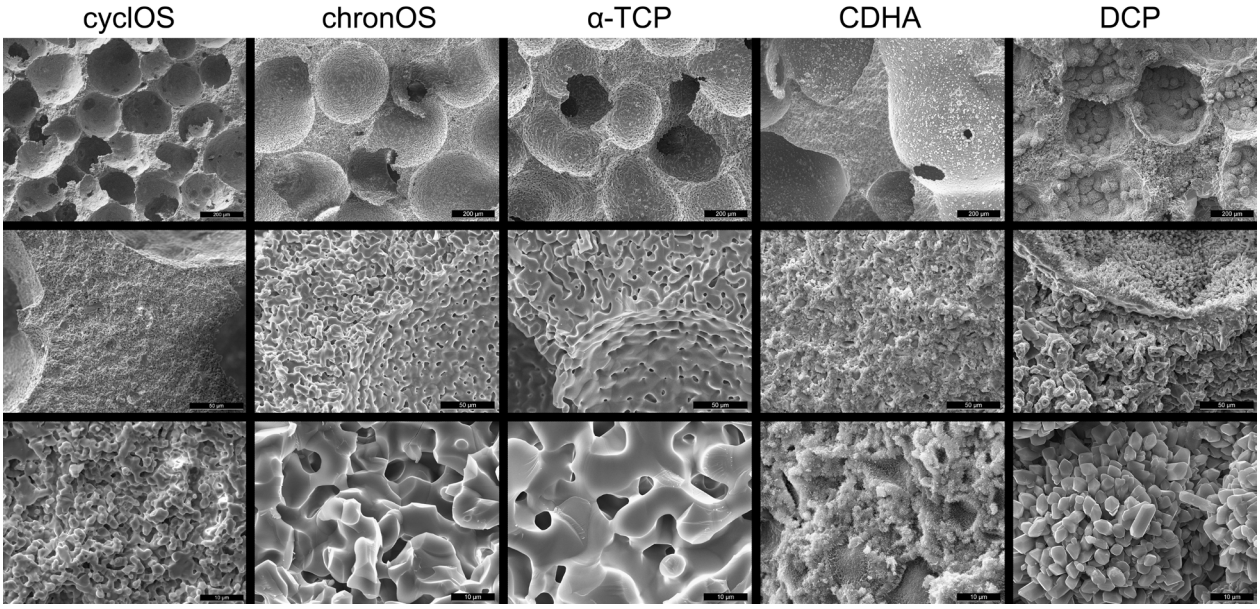

Fig. 1. SEM images of the 5 investigated CaP scaffold types. Three enlargements were used per material, from a small enlargement (images on top; scale bar: 200 µm) to a more detailed analysis of broken surfaces (images at the bottom; scale bar: 10 µm). The intermediate enlargements (middle images) have a scale bar of 50 µm.

Table 1. Summary of the physico-chemical properties of the samples used in the present study. Crystalline composition (Rietveld refinement analysis of the XRD data), specific surface area (SSA), macropore diameter, apparent density, porosity, median pore size (d50) and porosity accessible by bacteria (> 1.5 µm) in mean and standard deviation.

Material	Composition	Specific surface area [m^2/g]	Macropore Diameter [mm]	App Density [g/cm^3]	Porosity [%]	Porosity* [%]	Porosity accessible by bacteria (> 1.5 µm) * [%]	d_{50} * [µm]
β-TCP (chronOS)	>99 %[1)]	0.32 ± 0.01	0.39 ± 0.09	0.84 ± 0.03	72.6 ± 1.0	68 ± 3	59 ± 3	16 ± 3
β-TCP (cyclOS)	>99 %[2)]	0.84 ± 0.15	0.26 ± 0.07	0.88 ± 0.03	71.1 ± 1.0	70 ± 3	59 ± 3	17 ± 3
α-TCP	>99 %	0.16 ± 0.10[3)]	0.41 ± 0.09	0.89 ± 0.02	68.9 ± 0.7	62 ± 1	61 ± 1	51 ± 4
DCP	93 % DCP, 6 % α-TCP, 1 % DCPD	4.04 ± 0.35	0.37 ± 0.08	1.17 ± 0.04	60.0 ± 1.4	46 ± 2	37 ± 2	27± 7
CDHA	98 % HA, 2 % DCP	43.6 ± 0.4	0.53 ± 0.13	0.53 ± 0.01	82.0 ± 0.3	69 ± 4	27 ± 9	0.23 ± 0.18

* Determined by mercury porosimetry
[1)]Crystallite size: 163 ± 34 nm (± 1 St Dev)
[2)]Crystallite size: 103 ± 12 nm (± 1 St Dev)
[3)]This value is at the lower range of what the instrument can measure

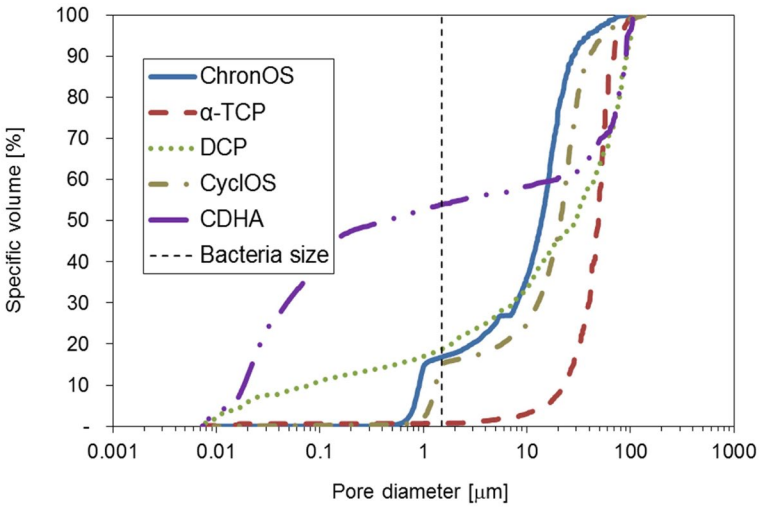

Fig. 2. Representative curves showing the normalised pore size distributions of the 5 investigated CaP scaffold types. The curves represent the fraction of the pores smaller than a given value. The vertical line corresponds to the approximate size of bacteria.

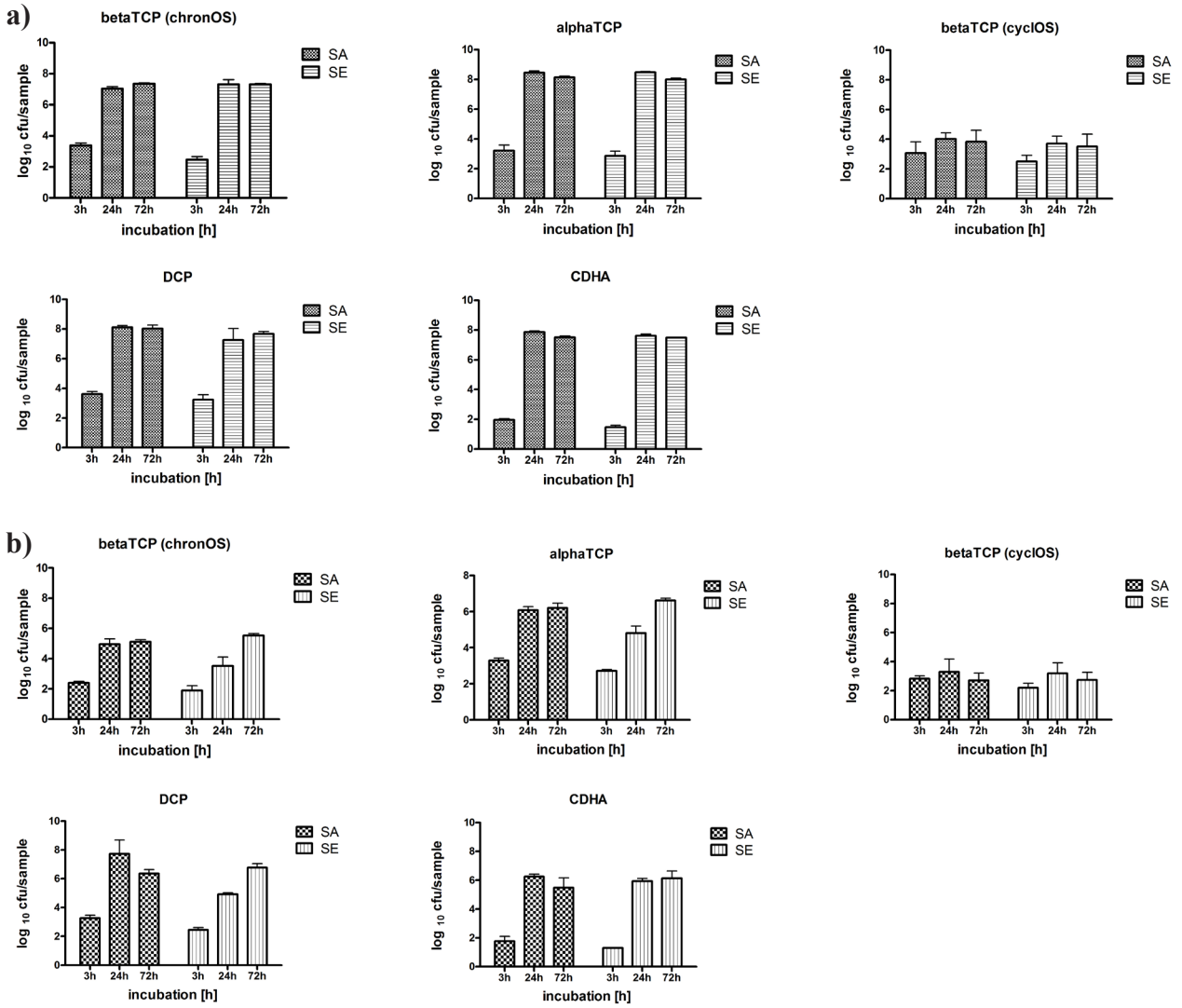

Fig. 3. The cfu count in sonication fluid of scaffolds incubated in (**a**) TSB and (**b**) serum (SA *S. aureus*, SE *S. epidermidis*). Data presented as mean ± SD.

to 0.2-0.6 mm and smaller pores, either in the nm (*e.g.*, for CHDA and DCP) or in the low μm range (1-10 μm) (Table 1, Fig. 1).

α-TCP and DCP scaffolds were produced from β-TCP scaffolds (chronOS), so their macropore size distribution and morphology were similar (Fig. 1; first row). However, the macropores of DCP samples were partly filled with small DCP protuberances, which led to a 10 % lower porosity and 5-10 % decrease in macropore size compared to β-TCP and α-TCP scaffolds (Table 1). The difference of microstructure seen on the SEM photos between the various scaffolds was reflected by large variations of SSA values. Indeed, the SSA values of the scaffolds varied over a very wide range, starting from 0.16 ± 0.10 m^2/g for α-TCP scaffolds up to 43.6 ± 0.4 m^2/g for CDHA scaffolds.

SEM images also revealed that CDHA samples had the largest macropore size (0.53 ± 0.13 mm), whereas cyclOS samples had the smallest macropore size (0.26 ± 0.07 mm). These observations were supported by the macropore size estimated from polished scaffold surfaces (Table 1). However, changes in macropore size remained small. Contrarily, large differences in micropore size were observed by SEM. Qualitatively, the mean pore size as determined by Hg porosimetry decreased in the order: α-TCP > chronOS > DCP > cyclOS > CDHA (Table 1).

Microstructure in terms of pore size distribution was further studied by Hg porosimetry to evaluate the possible bacteria invasion into the structure (Fig 2). Pore size distributions were normalised according to their volume in order to show the differences between scaffolds. According to these results, all materials but α-TCP had pores small enough to partly prevent bacterial invasion (estimated size of the two bacterial strains: 1.5 μm). Whereas the porosity fraction, not accessible to bacteria, was close to 80-87 % for chronOS, cyclOS and DCP, this value dropped to 39 % for CDHA scaffolds (= 27 %/69 %).

The porosities determined by Hg porosimetry were 1 to 14 % smaller than the values obtained *via* the determination of the geometrical density (Table 1). Whereas the differences were small for chronOS and cyclOS (4 % and 1 %), much larger differences were observed for DCP (14 %) and CDHA (13 %).

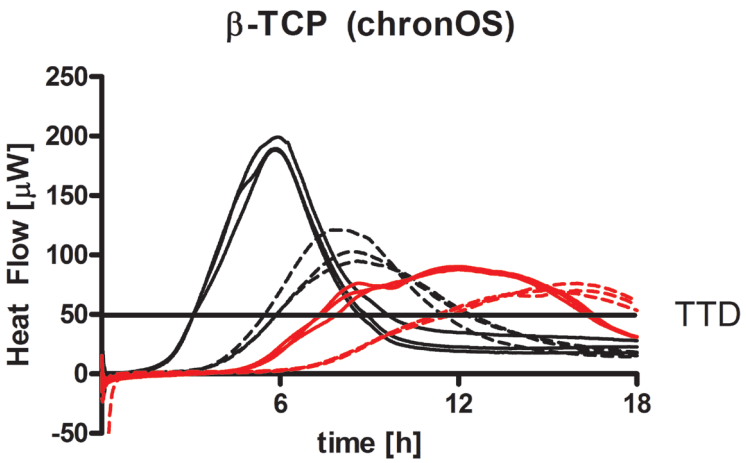

Fig. 4. microcalorimetric results from chronOS scaffolds incubated for 3 h with *S. aureus* and TSB (black line), *S. aureus* and serum (black dotted line), *S. epidermidis* and TSB (red line) and *S.*

Biofilm formation

Both test strains formed a biofilm on all test materials, as confirmed by quantitative culture after washing and sonication of the CaP scaffolds. The amount of biofilm removed from the scaffolds showed low variation within a triplicate and was comparable for 4 of the 5 tested materials, namely α-TCP, chronOS, CDHA and DCP but different for cyclOS (Fig. 3a,b).

For α-TCP, chronOS, CDHA and DCP incubated with *S. aureus* in TSB, differences between 3 h and 24 h ($p < 0.001$), 3 h and 24 h ($p < 0.001$) and 24 h and 72 h ($p > 0.05$) were comparable. The differences were the same when these 4 materials were incubated with *S. aureus* in serum, and when incubated with *S. epidermidis* in TSB (Fig. 3).

For cyclOS incubated with *S. aureus* in TSB, differences were less marked between 3 h and 24 h ($p < 0.01$), 3 h and 24 h ($p < 0.05$) and 24 h and 72 h ($p > 0.05$). When cyclOS was incubated in serum there were no significant differences ($p > 0.05$) between the 3 time points (Fig. 3a).

When the 5 materials were incubated with *S. epidermidis* in serum, again no significant differences ($p > 0.05$) were found between the 3 time points for cyclOS, but a continuous and highly significant increase was noticed between 3 h and 24 h for α-TCP ($p < 0.001$), chronOS ($p < 0.01$), CDHA ($p < 0.001$), and DCP ($p < 0.001$), and between 24 h and 72 h for α-TCP ($p < 0.001$), chronOS ($p < 0.001$), and DCP ($p < 0.001$) (Fig. 3b).

The qualitative analysis of the biofilm showed a homogenous size of CFU in the sonication fluid for all samples without contaminations on the plates.

The triplicates in microcalorimetric measurements showed a high uniformity of the shape of the curves (indicating no gross contamination on the scaffolds) with low variations in TTD, independent from the strain, growth medium, and length of incubation (Fig. 4). When these findings are combined with the qualitative analysis of the sonication fluid, contaminations on the samples can be excluded.

The lowest number of bacteria (longest TTD) was found on the surface of the CDHA scaffolds ($p < 0.001$ *S. aureus* and *S. epidermidis*) after 3 h incubation in TSB (Fig. 5a). The differences decreased after 24 h incubation ($p > 0.05$ *S.aureus*, $p < 0.05$ *S. epidermidis*) and disappeared after 72 h incubation ($p > 0.05$). When incubated in serum, there was significantly less biofilm on the surface of the CDHA and the cyclOS scaffolds as compared to the three other samples after 3 h incubation ($p < 0.001$). After 24 h and 72 h incubation cyclOS showed the lowest amount of biofilm (Fig. 5).

When the samples from group A (washing) and group B (washing and sonication) were compared less biofilm (longer TTD) was detected on the surface of all samples, but no change in the relative differences between the materials, time-points, and media (Fig. 5). All materials showed less biofilm (longer TTD) at corresponding time points when incubated in serum as compared to TSB (Fig. 5).

The amount of biofilm detected by microcalorimetry (TTD) for group A (washing) and B (washing and sonication) correlated well with the cfu counts after sonication.

Discussion

Numerous studies have been devoted to the quest of an ideal bone scaffold design (pore size, interconnectivity, shape, stability) without giving a clear answer (Bohner *et al.*, 2011). Furthermore, depending on the clinical application, these specifications might vary. Design modifications may not only change bony ingrowth and substitution with time (Bohner *et al.*, 2011) but also influence bacterial adhesion and the related risk of infection (Clauss *et al.*, 2013) because they use the same adhesive mechanisms (Busscher *et al.*, 2012). From a clinical perspective, initial bacterial colonisation, competing with tissue cell integration, better known as the "race to the surface" (Gristina, 1987), is the most important step as it preludes biomaterial associated infection (Busscher *et al.*, 2012).

Extensive research has been performed to determine the propensity of medical devices to sustain biofilm formation by staphylococci (Busscher *et al.*, 2012; Clauss *et al.*, 2010; Harris and Richards, 2006). It has been shown, that various physico-chemical factors influence *in vitro* biofilm formation on a surface (Harris *et al.*, 2007; Jakubowski

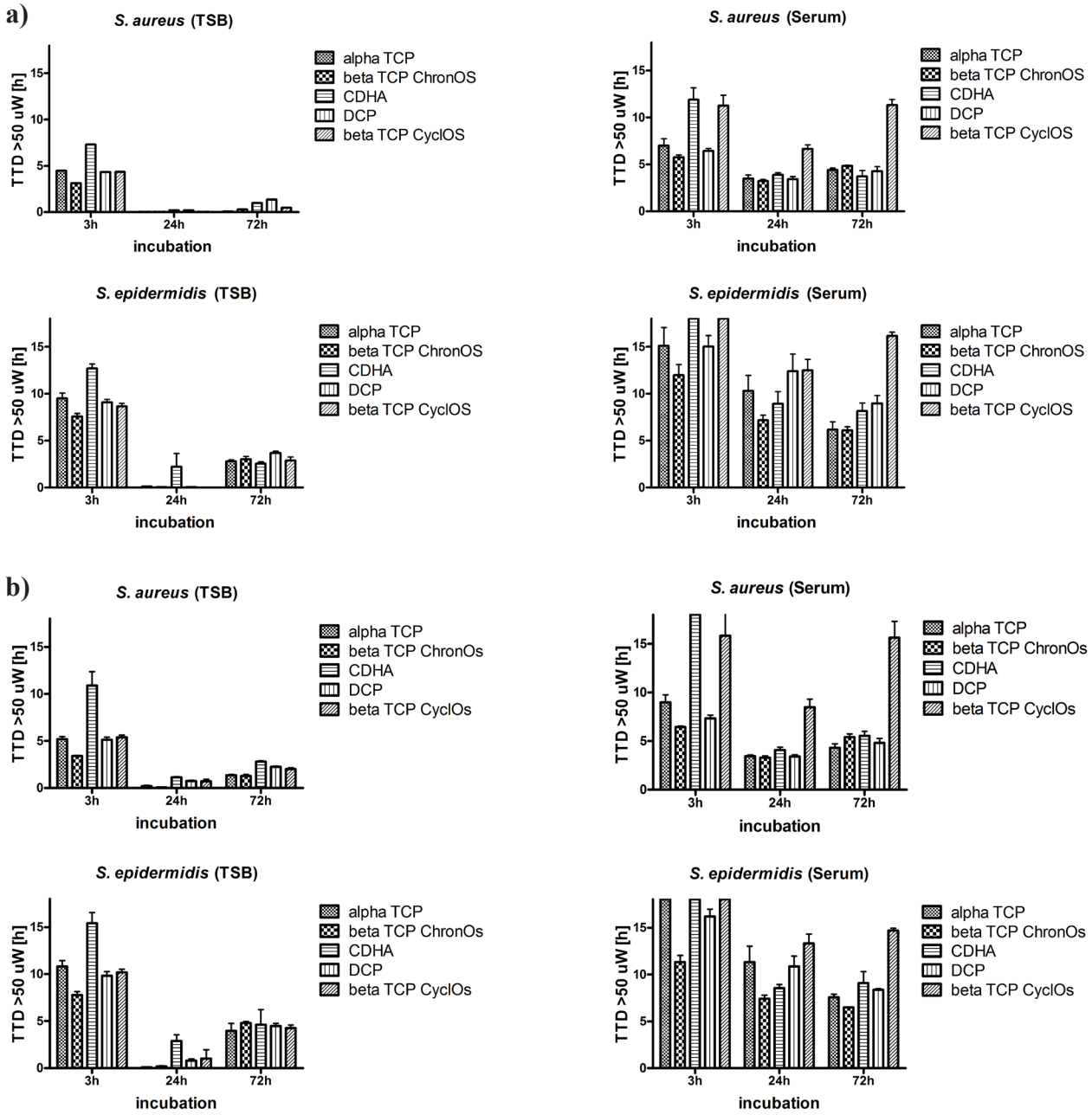

Fig. 5. Results from microcalorimetry. (**a**) washing procedure (group A), (**b**) washing and sonication (group B). Data presented as mean ± SD.

et al., 2008; MacKintosh *et al.*, 2006; Oga *et al.*, 1988; Patel *et al.*, 2003; Patel *et al.*, 2007). There is only limited information about staphylococcal biofilm formation on the surface of CaP bone grafts investigating *S. aureus* biofilm formation on either HA (Van Blitterswijk *et al.*, 1986a; Van Blitterswijk *et al.*, 1986b) or β-TCP (Van Blitterswijk *et al.*, 1986c) in the middle ear of rats.

The aim of this study was to analyse the influence of physico-chemical and structural variations of CaP bone grafts on staphylococcal biofilm formation under standardised *in vitro* conditions.

Several CaP materials were selected based on their clinical and scientific relevance. Nowadays, β-TCP is perhaps the most commonly used CaP bone graft substitute (Bohner, 2010). Therefore, two β-TCP scaffolds used clinically were considered. These two materials present very similar pore architectures. In both cases, the pores are spherical, the porosity is close to 70 %, and the structure is highly microporous (Figs. 1 and 2). The specific surface area is larger, whereas the macropores are slightly smaller and less interconnected for cyclOS compared to chronOS. CDHA is generally not used as scaffold due to its more complex manufacturing process (Steffen *et al.*, 2001; Kasten *et al.*, 2003), but since it is the end product of the setting reaction of many calcium phosphate cements, it is a relevant material. Also, CDHA is a very interesting material to analyse considering the importance of surfaces for bacterial biofilms. Indeed, its specific surface area is several orders of magnitude larger than that of β-TCP and α-TCP scaffolds (Table 1). Whereas CDHA and β-TCP

solubilities are very similar, the two last materials, *i.e.*, DCP and α-TCP, have a much higher solubility (Chow, 1991), which may affect their bacterial reaction. Furthermore, DCP is considered to be one of the most promising bone graft substitute materials (Habibovic *et al.*, 2008; Bohner, 2010).

All scaffolds are composed of pores large enough and interconnected enough to allow the invasion of bacteria (Ø 0.5-1.5 μm) into the structure. However, differences can be found between scaffolds: whereas only 39 % of CDHA porosity can be invaded by 1.5 μm spheres, this value increases to 80-87 % for DCP, chronOS and cyclOS, and reaches 100 % for α-TCP.

The two scaffold types with the lowest porosity accessible by bacteria (CDHA and DCP) are also the scaffolds with the highest SSA values and presenting the largest differences between the porosity inferred from the geometrical density and from Hg porosimetry measurements. These results suggest that CDHA and DCP scaffolds are partly crushed during Hg impregnation, hence leading to an overestimation of the total porosity, and an error in the porosity fraction smaller than 1.5 μm. Indeed, the scaffolds used in the present study have a compressive strength inferior to 10 MPa (particularly CDHA), which is the pressure required to invade 0.15 μm pores. At this pressure (or this pore size), only ≈50 % of the CDHA pores are invaded by Hg (and ≈90 % of the DCP pores).

Choosing the appropriate strain is one of the most crucial steps when biofilm formation is investigated. Clinical isolates are not well characterised and results might be difficult to compare to the literature. We therefore used standard (ATCC) strains which are known to produce reproducible amounts of biofilm already after 3 h for *S. aureus* (Ceri *et al.*, 1999) and *S. epidermidis* (Polonio *et al.*, 2001; Chaw *et al.*, 2005; Qin *et al.*, 2007), at the surface of various bone grafts (Clauss *et al.*, 2010; Clauss *et al.*, 2013).

Two different growth media (TSB and human serum) were chosen because it has been shown that growth media have a considerable influence on biofilm formation, as they change the initial bacterial adhesion on the surface (Barton *et al.*, 1996; Patel *et al.*, 2007). TSB was frequently used in previous studies (Clauss *et al.*, 2010; Clauss *et al.*, 2013), and additionally we used normal undiluted pooled human serum which was not heat-inactivated by the manufacturer. The presence of bacterial biofilms grown in serum proves that the two staphylococcal strains tested were able to survive and proliferate (more bacteria after 24 h and 72 h compared to 3 h of incubation). Compared to the dislodged biofilms that had been cultured in TSB (Fig. 3a), the biofilms grown in serum were slightly smaller (*i.e.*, lower cfu counts obtained). This could be explained by the fact that the TSB is a very nutrient-rich growth medium in comparison to serum. We believe that *in vitro* experiments performed in serum better represent the clinical setting, where the bacteria are present in a more challenging and harsh environment, compared to the nutrient-rich TSB.

The goal of this study was to investigate the effect of different physico-chemical material characteristics on staphylococcal biofilm formation, and not to compare different growth media. Therefore, we did not emphasise the difference in growth between the two culture media. An interesting observation was that less biofilm was found on the cyclOS scaffolds both when TSB and serum were used, which proved that the smaller amount of biofilm found on this particular material was not due to interaction between the growth media (TSB or serum) and the material.

Various methods for quantitative/qualitative evaluation of biofilm formation, like "live-dead staining", confocal laser scanning microscopy (CLSM) or SEM have been described. All methods except calorimetry need a special pre-treatment, such as staining (live-dead staining, CLSM) or carbon-sputtering (SEM), which interfere with further biofilm investigation (Clauss *et al.*, 2010). The surface that can be monitored by other methods is restricted to small areas while microcalorimetry monitors the whole device (Clauss *et al.*, 2010). For microcalorimetric monitoring of biofilm formation it is essential to remove planktonic bacteria from the scaffolds, and washing might be critical with porous materials such as CaP bone grafts. Planktonic bacteria might remain in the pores, resulting in an overestimation of the true amount of biofilm. To minimise this effect we modified our recently published washing protocol (Clauss *et al.*, 2010) for removal of planktonic bacteria. Uniformly, all samples were washed five times placing the suction device directly on top, and to one side, of the sample producing a flush through the scaffolds. We cannot quantify the amount of remaining planktonic bacteria but variations in cfu counts and TTD within a triplicate have been low, thus systematic error should be low and comparable on all scaffolds.

Several material parameters are known to modify the rate of infection *in vitro*. For example, porous materials have a higher rate of infection than dense materials (Merritt *et al.*, 1998; Harris *et al.*, 2007; Clauss *et al.*, 2010). Rough materials are also more prone to infection (Lange *et al.*, 2002; Meredith *et al.*, 2005). The investigated CaP bone grafts were porous, with a microscopically and macroscopically rough surface. The materials presented obvious but moderate differences in porosity and roughness, as revealed by SEM, Hg porosimetry, and nitrogen adsorption. Biofilm formation on the surface of the CaP samples by means of sonication and microcalorimetry was comparable for α-TCP, chronOS, CDHA and DCP, but much lower for cyclOS. This is peculiar because this calcium phosphate had an intermediate porosity (Table 1), mean pore size, specific surface area, and porosity accessible to bacteria. Therefore, it is unclear why cyclOS would be less prone to biofilm formation than the other materials.

Hydrophobicity has been shown to be an important factor for initial bacterial adhesion and *E. coli* biofilm formation on the surface of HA and β-TCP (Jakubowski *et al.*, 2008).

In the past, Staehli *et al*. had shown that cyclOS samples were more difficult to impregnate by a fluid than chronOS (Stähli *et al.*, 2010), what might result in a higher volume of air in the cyclOS samples reducing the surface available for biofilm formation. They established an impregnation test setup and assessed the effect of various synthesis parameters, such as sintering temperature, composition, macroporosity and macropore size on the impregnation

properties of porous CaP scaffolds dipped in water. Among those parameters, the macropore size had by far the largest effect; generally, the bigger the macropore size, the lower the saturation level. The results also showed that impregnation was less complete when the samples were fully dipped in water than when they were only partially dipped, owing to the requirement for the system to create air bubbles under water. We were not able to modify pore size of the samples as this was one of our major issues in the present study, but we placed the scaffolds on top of the surface of the liquid allowing them to submerge within 30 min, wetting just as much surface as possible. One would also expect that the effect of entrapped air should reduce with time, thus the influence on the results should become smaller from the 3 h to 24 h and 72 h incubation. As differences in biofilm formation became more obvious by longer incubation intervals, differences in impregnation can most likely not explain the observed differences in biofilm formation. Besides hydrophobicity, bacterial adhesion can also be influenced by the charge of the surface, *i.e.*, negatively charged bacteria adhere better to a positively charged surface (Li and Logan, 2004). We did not investigate surface charge, thus we cannot exclude that surface charge influenced our results.

Conclusion

All investigated CaP bone grafts showed significant amounts of biofilm on the surface already after 24 h. CyclOS had the lowest biofilm formation, but this difference cannot be explained rationally based on the physico-chemical characterisations such as pore size distribution, porosity, specific surface area. Our results suggest that biofilm formation is not influenced by a single physico-chemical parameter alone, but is a multi-step process influenced by several factors in parallel. Further studies are needed to decipher the whole cascade. Infections on the surface of medical devices are mainly acquired perioperative, thus a high resistance against initial bacterial adhesion and biofilm formation is favourable to reducing infection rates with medical devices. Transfer from *in vitro* data to the clinical situation is difficult. As there might be various reasons for reduced biofilm formation on cyclOS scaffolds, compared with the four other CaP bone grafts, we believe that advocating cyclOs in clinical situations with a high risk of infection such as *e.g.*, open fractures, cannot clearly be supported based on our data.

Acknowledgements

This study was supported by research grants from the RMS Foundation; Bettlach, Switzerland (E09_0001), the Swiss Society of Orthopaedics and Traumatology (SGOT/SSOT) and 3R Foundation (S124-10). *S. epidermidis* RP62A (ATCC 35984) was kindly provided by Prof. P. Vaudaux from the Department of Infectious Disease, University Hospital, Geneva, Switzerland. At the RMS Foundation we want to thank S. Grünefelder and P. Brotschi for their help producing the scaffolds, W. Hirsinger for his help with the SEM studies and L. Galea for the BET and XRD analysis. Furthermore we have to thank S. Gersbach (Kantonsspital Baselland Liestal) for her help with data management and analysis.

References

Barton AJ, Sagers RD, Pitt WG (1996) Bacterial adhesion to orthopedic implant polymers. J Biomed Mater Res **30**: 403-410.

Bohner M (2000) Calcium orthophosphates in medicine: from ceramics to calcium phosphate cements. Injury **31 Suppl 4**: 37-47.

Bohner M (2001) Calcium phosphate emulsions: possible applications. Key Eng Mater **192-195**: 765-768.

Bohner M (2010) Resorbable biomaterials as bone graft substitutes. Mat Today **13**: 24-30.

Bohner M, Van Lenthe GH, Grünenfelder S, Hirsiger W, Evison R, Müller R (2005) Synthesis and characterization of porous beta-tricalcium phosphate blocks. Biomaterials **26**: 6099.

Bohner M, Loosli Y, Baroud G, Lacroix D (2011) Commentary: Deciphering the link between architecture and biological response of a bone graft substitute. Acta Biomater **7**: 478-484.

Busscher HJ, van der Mei HC, Subbiahdoss G, Jutte PC, van den Dungen JJ, Zaat SA, Schultz MJ, Grainger DW (2012) Biomaterial-associated infection: locating the finish line in the race for the surface. Sci Transl Med **4**: 153rv110.

Ceri H, Olson M, Morck D, Storey D, Read R, Buret A, Olson B (2001)The MBEC assay system: Multiple equivalent biofilms for antibiotic and biocide susceptibility testing. In: Methods Enzymol **337**: 377-385.

Ceri H, Olson ME, Stremick C, Read RR, Morck D, Buret A (1999) The Calgary Biofilm Device: New technology for rapid determination of antibiotic susceptibilities of bacterial biofilms. J Clin Microbiol **37**: 1771-1776.

Chaw KC, Manimaran M, Tay FEH (2005) Role of silver ions in destabilization of intermolecular adhesion forces measured by atomic force microscopy in *Staphylococcus epidermidis* biofilms. Antimicrob Agents Chemother **49**: 4853-4859.

Chow LC (1991) Development of self-setting calcium phosphate cements. Japan Ceram Soc **99**: 954-964.

Clauss M, Trampuz A, Borens O, Bohner M, Ilchmann T (2010) Biofilm formation on bone grafts and bone graft substitutes: comparison of different materials by a standard *in vitro* test and microcalorimetry. Acta Biomater **6**: 3791-3797.

Clauss M, Tafin UF, Bizzini A, Trampuz A, Ilchmann T (2013) Biofilm formation by staphylococci on fresh, fresh-frozen and processed human and bovine bone grafts. Eur Cell Mater **25**: 159-166.

Cordero J, Munuera L, Folgueira MD (1994) Influence of metal implants on infection. An experimental study in rabbits. J Bone Joint Surg Br **76**: 717-720.

Costerton JW, Montanaro L, Arciola CR (2005) Biofilm in implant infections: its production and regulation. Int J Artif Organs **28**: 1062-1068.

Crockarell JR, Hanssen AD, Osmon DR, Morrey BF (1998) Treatment of infection with debridement and retention of the components following hip arthroplasty. J Bone Joint Surg Am **80**: 1306-1313.

Curry NA, Jones DW (1971) Crystal structure of brushite, calcium hydrogen orthophosphate dihydrate: a neutron diffraction investigation. J Chem Soc (A) Inorg Phys Theor **1971**: 3725-3729.

Delloye C, Cornu O, Druez V, Barbier O (2007) Bone allografts: What they can offer and what they cannot. J Bone Joint Surg Br **89**: 574-579.

Dickens B, Bowen JS, Brown BE (1971) A refinement of the crystal structure of CaHPO4 (synthetic monetite). Acta Cryst **B28**: 797-806.

Dickens B, Schroeder LW, Brown BE (1974) Crystallographic studies of the role of Mg as a stabilizing impurity in β-$Ca_3(PO_4)_2$. I. The crystal structure of pure β-$Ca_3(PO_4)_2$. J Solid State Chem **10**: 232-248.

Ehrlich GD, Stoodley P, Kathju S, Zhao Y, McLeod BR, Balaban N, Hu FZ, Sotereanos NG, Costerton JW, Stewart PS, Post JC, Lin Q (2005) Engineering approaches for the detection and control of orthopaedic biofilm infections. Clin Orthop Relat Res **437**: 59-66.

Galea LG, Bohner M, Lemaitre J, Kohler T, Muller R (2008) Bone substitute: transforming beta-tricalcium phosphate porous scaffolds into monetite. Biomaterials **29**: 3400-3407.

Gristina AG (1987) Biomaterial-centered infection: Microbial adhesion *versus* tissue integration. Science **237**: 1588-1595.

Habibovic P, Gbureck U, Doillon CJ, Bassett DC, van Blitterswijk CA, Barralet JE (2008) Osteoconduction and osteoinduction of low-temperature 3D printed bioceramic implants. Biomaterials **29**: 944-953.

Harris LG, Richards RG (2006) Staphylococci and implant surfaces: a review. Injury **37 Suppl 2**: S3-14.

Harris LG, Meredith DO, Eschbach L, Richards RG (2007) *Staphylococcus aureus* adhesion to standard micro-rough and electropolished implant materials. J Mater Sci: Mater Med **18**: 1151-1156.

Jakubowski W, lósarczyk A, Paszkiewicz Z, Szymanski W, Walkowiak B (2008) Bacterial colonisation of bioceramic surfaces. Adv Appl Ceram **107**: 217-222.

Kappe T, Cakir B, Mattes T, Reichel H, Flören M (2010) Infections after bone allograft surgery: a prospective study by a hospital bone bank using frozen femoral heads from living donors. Cell Tissue Banking **11**: 253-259.

Kasten P, Luginbuhl R, van Griensven M, Barkhausen T, Krettek C, Bohner M, Bosch U (2003) Comparison of human bone marrow stromal cells seeded on calcium-deficient hydroxyapatite, beta-tricalcium phosphate and demineralized bone matrix. Biomaterials **24**: 2593-2603.

Ketonis C, Barr S, Adams CS, Hickok NJ, Parvizi J (2010) Bacterial colonization of bone allografts: establishment and effects of antibiotics. Clin Orthop Relat Res **468**: 2113-2121.

Lange R, Luthen F, Beck U, Rychly J, Baumann A, Nebe B (2002) Cell-extracellular matrix interaction and physico-chemical characteristics of titanium surfaces depend on the roughness of the material. Biomol Eng **19**: 255-261.

Li B, Logan BE (2004) Bacterial adhesion to glass and metal-oxide surfaces. Colloids Surf B Biointerfaces **36**: 81-90.

MacKintosh EE, Patel JD, Marchant RE, Anderson JM (2006) Effects of biomaterial surface chemistry on the adhesion and biofilm formation of *Staphylococcus epidermidis in vitro*. J Biomed Mater Res A **78**: 836-842.

Mathew M, Schroeder LW, Dickens B, Brown WE (1977) The crystal structure of a-$Ca_3(PO_4)_2$. Acta Cryst **B33**: 1325-1333.

Meredith DO, Eschbach L, Wood MA, Riehle MO, Curtis AS, Richards RG (2005) Human fibroblast reactions to standard and electropolished titanium and Ti-6Al-7Nb, and electropolished stainless steel. J Biomed Mater Res A **75**: 541-555.

Merritt K, Gaind A, Anderson JM (1998) Detection of bacterial adherence on biomedical polymers. J Biomed Mater Res **39**: 415-422.

Oga M, Sugioka Y, Hobgood CD, Gristina AG, Myrvik QN (1988) Surgical biomaterials and differential colonization by *Staphylococcus epidermidis*. Biomaterials **9**: 285-289.

Ostermann PA, Henry SL, Seligson D (1994) Timing of wound closure in severe compound fractures. Orthopedics **17**: 397-399.

Patel JD, Ebert M, Stokes K, Ward R, Anderson JM (2003) Inhibition of bacterial and leukocyte adhesion under shear stress conditions by material surface chemistry. J Biomater Sci Polym Ed **14**: 279-295.

Patel JD, Ebert M, Ward R, Anderson JM (2007) *S. epidermidis* biofilm formation: Effects of biomaterial surface chemistry and serum proteins. J Biomed Mater Res A **80**: 742-751.

Polonio RE, Mermel LA, Paquette GE, Sperry JF (2001) Eradication of biofilm-forming *Staphylococcus epidermidis* (RP62A) by a combination of sodium salicylate and vancomycin. Antimicrob Agents Chemother **45**: 3262-3266.

Qin Z, Yang X, Yang L, Jiang J, Ou Y, Molin S, Qu D (2007) Formation and properties of *in vitro* biofilms of ica-negative *Staphylococcus epidermidis* clinical isolates. J Med Microbiol **56**: 83-93.

Rodriguez-Carvajal J (2001) Recent Developments of the Program FULLPROF. Commission on Powder Diffraction (IUCr) Newsletter **26**: 12-19.

Schlegel U, Perren SM (2006) Surgical aspects of infection involving osteosynthesis implants: implant design and resistance to local infection. Injury **37 Suppl 2**: S67-73.

Stähli C, Bohner M, Bashoor-Zadeh M, Doebelin N, Baroud G (2010) Aqueous impregnation of porous beta-tricalcium phosphate scaffolds. Acta Biomater **6**: 2760-2772.

Steffen T, Stoll T, Arvinte T, Schenk RK (2001) Porous tricalcium phosphate and transforming growth factor used for anterior spine surgery. Eur Spine J **10 Suppl 2**: S132-140.

Sudarsanan K, Young RA (1969) Significant precision in crystal structure details: Holly springs hydroxyapatite. Acta Cryst **B25**: 1534-1543.

Tadic D, Epple M (2004) A thorough physicochemical characterisation of 14 calcium phosphate-based bone

substitution materials in comparison to natural bone. Biomaterials **25**: 987-994.

Trampuz A, Zimmerli W (2006a) Antimicrobial agents in orthopaedic surgery: Prophylaxis and treatment. Drugs **66**: 1089-1105.

Trampuz A, Zimmerli W (2006b) Diagnosis and treatment of infections associated with fracture-fixation devices. Injury **37 Suppl 2**: S59-66.

Van Blitterswijk CA, Bakker D, Grote JJ, Daems ThW (1986a) The biological performance of calcium phosphate ceramics in an infected implantation site: II. Biological evaluation of hydroxyapatite during short-term infection. J Biomed Mater Res **20**: 1003-1015.

Van Blitterswijk CA, Grote JJ, De Groot K (1986b) The biological performance of calcium phosphate ceramics in an infected implantation site: I. Biological performance of hydroxyapatite during *Staphylococcus aureus* infection. J Biomed Mater Res **20**: 989-1002.

Van Blitterswijk CA, Grote JJ, Koerten HK, Kuijpers W (1986c) The biological performance of calcium phosphate ceramics in an infected implantation site III: Biological performance of β-whitlockite in the noninfected and infected rat middle ear. J Biomed Mater Res **20**: 1197-1217.

Van de Pol GJ, Sturm PDJ, Van Loon CJ, Verhagen C, Schreurs BW (2007) Microbiological cultures of allografts of the femoral head just before transplantation. J Bone Joint Surg B **89**: 1225-1228.

Vogely HC, Oosterbos CJ, Puts EW, Nijhof MW, Nikkels PG, Fleer A, Tonino AJ, Dhert WJ, Verbout AJ (2000) Effects of hydroxyapatite coating on Ti-6A1-4V implant-site infection in a rabbit tibial model. J Orthop Res **18**: 485-493.

Westas E, Gillstedt M, Lonn-Stensrud J, Bruzell E, Andersson M (2014) Biofilm formation on nanostructured hydroxyapatite-coated titanium. J Biomed Mater Res A **102**: 1063-1070.

Discussion with Reviewers

T. Moriarty: Whilst accepting the authors' statement that extrapolation of *in vitro* data to the clinical situation is difficult, the results presented in this study nevertheless reveal a measured difference in bacterial biofilm formation between the test materials. This begs the question "How much importance should a clinician place on these results?". Are the authors able to draw on any examples of *in vitro* data of bacterial adhesion or biofilm formation on any material that has successfully been linked with clinical infection?

Authors: The reviewer raises two important points: First concerning the clinical relevance of our presented data. In the initial submission we draw the conclusion that the use of cyclOS can be advocated from the *in vitro* data. We toned down this statement due to the fact that so far *in vivo* data are missing (Geurts *et al.*, 2011, additional reference). However, it seems reasonable to use cyclOS instead of another tested CaP scaffold in cases with an increased risk of infection.

Concerning the second point, we recently published data on infection rates, biofilm formation and recurrence rates after lesser toe surgery comparing stainless steel and titanium Kirschner wires and were able to show superior results (lower recurrence rates, less biofilm formation, less clinical infections) for the titanium wires (Clauss *et al.*, 2013). These data confirm the *in vitro* (Arens *et al.*, 1996; Harris *et al.*, 2007, additional references) and animal experimental findings (Harris *et al.*, 2007, text reference; Melcher *et al.*, 1996; Johansson *et al.*, 1999; Sheehan *et al.*, 2004; Moriarty *et al.*, 2009, additional references) published for these two materials. Furthermore we found some evidence that clinical infection on cerebrospinal fluid catheters is comparable to *in vitro* and *in vivo* data (Bayston and Lambert, 1997; Pattavilakom *et al.*, 2006, additional references).

However, the question remains "How much importance should a clinician place on *in vitro* data or results obtained from animal models?" In a recent review on *S. aureus* osteomyelitis and animal models published, the authors clearly showed the limitations of various animal models concerning the transfer from animal data to the clinical situation (Reizner *et al.*, 2014). We think that choosing a certain material instead of another will not solely solve the problem of implant-associated infections alone but might be one step in reducing the number of infections.

T. Moriarty: In some clinical studies it has emerged that a significant proportion of bacteria that cause device-related infections are weak biofilm formers *in vitro*, yet are capable of causing biofilm infections on indwelling devices in human patients. Do the authors have any comment on this, or any data from tests of their materials with weak biofilm forming strains?

Authors: Biofilm formation is a multi-step process with some of these steps even running in parallel. The amount of biofilm formed on the surface thus is not only dependent to the capability of a bacterial strain to form biofilm or not but also on the specific environment. We do not have any additional *in vitro* data on biofilm formation with weak biofilm forming strains on the surface of the investigated CaP scaffolds.

Additional References

Arens S, Schlegel U, Printzen G, Ziegler WJ, Perren SM, Hansis M (1996) Influence of materials for fixation implants on local infection. An experimental study of steel *versus* titanium DCP in rabbits. J Bone Joint Surg Br **78**: 647-651.

Bayston R, Lambert E (1997) Duration of protective activity of cerebrospinal fluid shunt catheters impregnated with antimicrobial agents to prevent bacterial catheter-related infection. J Neurosurg **87**: 247-251.

Clauss M, Graf S, Gersbach S, Hintermann B, Ilchmann T, Knupp M (2013) Material and biofilm load of K wires in toe surgery: titanium *versus* stainless steel. Clin Orthop Relat Res **471**: 2312-2317.

Geurts J, Chris Arts JJ, Walenkamp GH (2011) Bone graft substitutes in active or suspected infection. Contra-indicated or not? Injury **42 Suppl 2**: S82-86.

Johansson A, Lindgren JU, Nord CE, Svensson O (1999) Local plate infections in a rabbit model. Injury **30**: 587-590.

Melcher GA, Hauke C, Metzdorf A, Perren SM, Printzen G, Schlegel U, Ziegler WJ (1996) Infection after intramedullary nailing: an experimental investigation on rabbits. Injury **27 Suppl 3**: SC23-26.

Moriarty TF, Debefve L, Boure L, Campoccia D, Schlegel U, Richards RG (2009) Influence of material and microtopography on the development of local infection *in vivo*: experimental investigation in rabbits. Int J Artif Organs **32**: 663-670.

Pattavilakom A, Kotasnas D, Korman TM, Xenos C, Danks A (2006) Duration of *in vivo* antimicrobial activity of antibiotic-impregnated cerebrospinal fluid catheters. Neurosurgery **58**: 930-935.

Reizner W, Hunter JG, O'Malley NT, Southgate RD, Schwarz EM, Kates SL (2014) A systematic review of animal models for *Staphylococcus aureus* osteomyelitis. Eur Cell Mater **27**: 196-212.

Sheehan E, McKenna J, Mulhall KJ, Marks P, McCormack D (2004) Adhesion of Staphylococcus to orthopaedic metals, an *in vivo* study. J Orthopaed Res **22**: 39-43.